

**" Sixth Workshop on Non-Linear Dynamics and
Earthquake Prediction"**

15 - 27 October 2001

**Model of Block Structure Dynamics and its Application to
Study Lithosphere Block Dynamics and Seismicity**

A. Soloviev

**International Institute of Earthquake Prediction Theory
and Mathematical Geophysics,
Russian Academy of Sciences
Moscow, Russia
www.mitp.ru**

*Model of Block Structure Dynamics and Its Application to
Study Lithosphere Block Dynamics and Seismicity*

A.Soloviev

**International Institute of Earthquake Prediction
Theory and Mathematical Geophysics
Russian Academy of Sciences
Warshavskoye sh. 79, kor. 2, Moscow 113556
Russian Federation
www.mitp.ru**

ABSTRACT

A model of block structure dynamics (or simpler "block model") considers a seismic region as a system of perfectly rigid blocks divided by infinitely thin plane faults. The blocks interact between themselves and with the underlying medium. The system of blocks moves as a consequence of prescribed motion of the boundary blocks and of the underlying medium. As the blocks are perfectly rigid, all deformation takes place in the fault zones and at the block base in contact with the underlying medium. Relative block displacements take place along the fault planes. This assumption is justified by the fact that for the lithosphere the effective elastic moduli of the fault zones are significantly smaller than those within the blocks. Block motion is defined so that the system is in a quasistatic equilibrium state. The interaction of blocks along the fault planes is viscous-elastic ("normal state") while the ratio of the stress to the pressure remains below a certain strength level. When the critical level is exceeded in some part of a fault plane, a stress-drop ("failure") occurs (in accordance with the dry friction model), possibly causing failure in other parts of the fault planes. These failures produce earthquakes. Immediately after the earthquake and for some time after, the affected parts of the fault planes are in a state of creep. This state differs from the normal state because of a faster growth of inelastic displacements, lasting until the stress falls below some other level. This modeling gives rise a synthetic earthquake catalogue.

Application of the model to study lithosphere block dynamics and seismicity enables to study relations between geometry of faults and block movements and earthquake flow, to reproduce some features of seismicity observed in a region under consideration, and to reconstruct tectonic driving forces from spatial distribution of seismicity. Clustering of earthquakes and dependence of the occurrence of large earthquakes on fragmentation of the media and on rotation of blocks were found in the model. These results are juxtaposed and analysed.

I. INTRODUCTION

Study of seismicity with the statistical and phenomenological analysis of the real earthquake catalogs has the disadvantage that the instrumental observation data cover, in general, a time interval of about one hundred years or even less. This time interval is very short, in comparison with the duration of tectonic processes responsible of the seismic activity. Therefore the patterns of the earthquake occurrence identifiable in a real catalog may be only apparent and may not repeat in the future. On the other hand the synthetic catalog obtained by numerical modeling of the seismogenetic process may cover very long time interval that allows us to acquire a more reliable estimation of the parameters of seismic flow.

Seismic observations show that features of a seismic flow are different for various active regions (e.g., Hattori 1974; Kronrod 1984; Molchan et al. 1997). It is natural to assume that this difference is due among other factors to contrasts in the tectonic structure of the regions and in main tectonic movements determining the lithosphere dynamics in the regions. If a single factor is considered, it is rather difficult if not impossible to detect and to single out its impact on features of an earthquake flow by analysis of seismic observations, because seismicity is controlled by an assemblage of factors some of which could be larger than one under consideration. This can be overcome by numerical modeling of the processes generating seismicity and studying synthetic earthquake catalogs obtained (e.g., Shaw et al. 1992; Gabrielov and Newman 1994; Allègre et al. 1995; Newman et al. 1995; Turcotte 1997; Narteau et al. 2000).

Mathematical models of lithosphere dynamics are also tools for the study of the earthquake preparation process and useful in earthquake prediction studies (e.g., Gabrielov and Newman 1994). The model can be used also to suggest new premonitory patterns that might exist in real catalogs (e.g., Gabrielov et al. 2000; Shebalin et al. 2000).

The model of block structure dynamics exploits the hierarchical block structure of the lithosphere proposed by Alekseevskaya et al. (1977). The basic principles of the model are developed by Gabrielov et al. (1986, 1990) on the basis of the proposition that blocks of the lithosphere are separated by comparatively thin, weak and less consolidated fault zones, such as lineaments and tectonic faults, and major deformation and most earthquakes occur in such fault zones. Later on the model was improved to create possibility of approximating in it a block structure of a real seismoactive region under consideration (Soloviev 1995).

A seismic region is modeled by a system of absolutely rigid blocks divided by infinitely thin plane faults. This assumption is justified by the fact that for the lithosphere the effective elastic moduli of the fault zones are significantly smaller than those within the blocks. The blocks interact between themselves and with the underlying medium. The system of blocks moves as a consequence of prescribed motion of the boundary blocks and of the underlying medium.

As the blocks are absolutely rigid, all deformation takes place in the fault zones and at the block base in contact with the underlying medium. Relative block displacements take place along the fault planes. Block motion is defined so that the system is in a quasistatic equilibrium state.

The interaction of blocks along the fault planes is viscous-elastic ("normal state") while the ratio of the stress to the pressure remains below a certain strength level. When the critical level is exceeded in some part of a fault plane, a stress-drop ("failure") occurs (in accordance with the dry friction model), possibly causing failure in other parts of the fault planes. These failures produce earthquakes. Immediately after the earthquake and for some time after, the affected parts of the fault planes are in a state of creep. This state differs from the normal state because of a faster growth of inelastic displacements, lasting until the stress falls below some other level. This numerical modeling gives rise a synthetic earthquake catalog.

The major results obtained by means of the model of block structure dynamics are

juxtaposed and analyzed below. In particular they include possibility to reconstruct tectonic driving forces from epicenter distribution and other seismicity features. The model was studied to look for space-temporal correlation between synthetic earthquakes: clustering of synthetic earthquakes, the long-range interaction between them etc. Dependence of the occurrence of strong earthquakes on fragmentation of the media, and on rotation of blocks was analyzed. Dynamics and seismicity of an abstract arc subduction zone was modeled to study dependence of seismicity features on a dip angle of subduction zone and on direction of relative movement of continental and oceanic plates. Geometry of real faults and blocks was considered in block models of the Vrancea earthquake-prone region (Romania), of the Western Alps, and of Sunda Arc (Sunda Isles). The numerical experiments gave possibility to obtain the values of the model parameters supplying synthetic earthquake catalogs with the spatial distribution of epicenters and frequency-magnitude (FM) relation close to those of the observed seismicity in the region.

II. MODEL OF BLOCK STRUCTURE DYNAMICS

The definitions used in the block model and its formal mathematical description are given below.

2.1 Block Structure Geometry

A layer with thickness H limited by two horizontal planes is considered (Fig. 1), and a block structure is defined as a limited and simply connected part of this layer. Each lateral boundary of the block structure is defined by portions of the parts of planes intersecting the layer. The subdivision of the structure into blocks is performed by planes intersecting the layer. The parts of these planes, which are inside the block structure and its lateral faces, are called "fault planes".

The geometry of the block structure is defined by the lines of intersection between the fault planes and the upper plane limiting the layer (these lines are called "faults"), and by the angles of dip of each fault plane. Three or more faults cannot have a common point on the upper plane, and a common point of two faults is called "vertex". The direction is specified for each fault and the angle of dip of the fault plane is measured on the left of the fault. The positions of a vertex on the upper and the lower plane, limiting the layer, are connected by a segment ("rib") of the line of intersection of the corresponding fault planes. The part of a fault plane between two ribs corresponding to successive vertices on the fault is called "segment". The shape of the segment is a trapezium. The common parts of the block with the upper and lower planes are polygons, and the common part of the block with the lower plane is called "bottom".

It is assumed that the block structure is bordered by a confining medium, whose motion is prescribed on its continuous parts comprised between two ribs of the block structure boundary. These parts of the confining medium are called "boundary blocks".

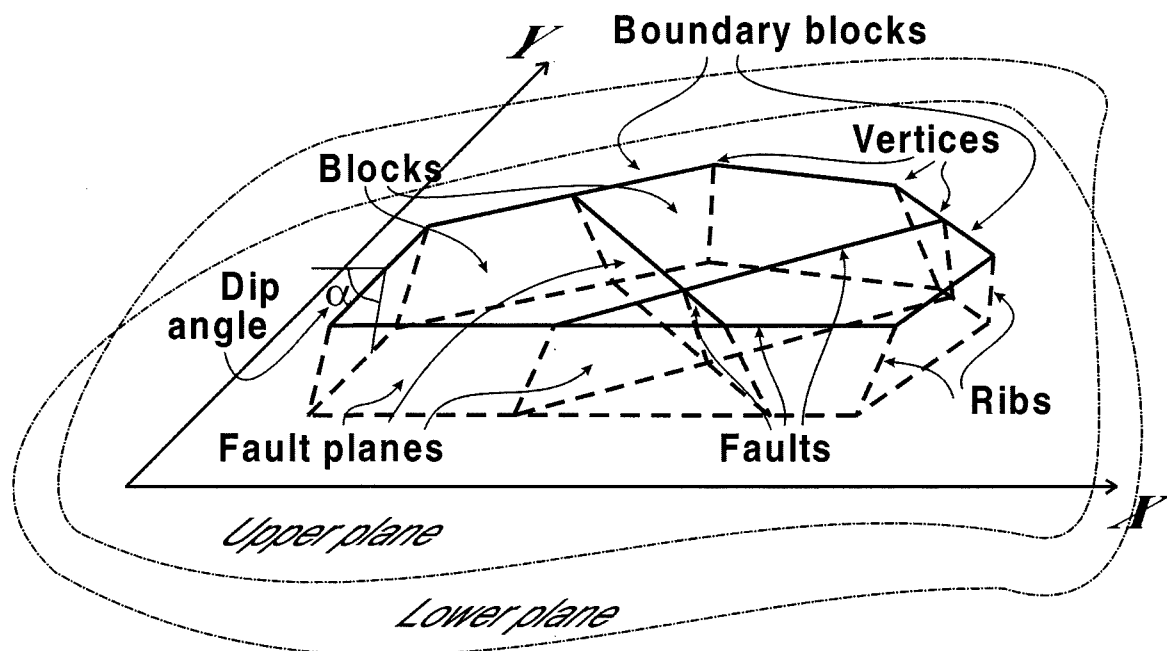


FIGURE 1 A sketch of a block model.

2.2 Block Movement

The blocks are assumed to be rigid and all their relative displacements take place along the bounding fault planes. The interaction of the blocks with the underlying medium takes place along the lower plane, any kind of slip being possible.

The movements of the boundaries of the block structure (the boundary blocks) and the medium underlying the blocks are assumed to be an external force on the structure. The rates of these movements are considered to be horizontal and known.

Non-dimensional time is used in the model, therefore all quantities that contain time in their dimensions are referred to one unit of the non-dimensional time, and their dimensions do not contain time. For example, in the model, velocities are measured in units of length and the velocity of 5 cm means 5 cm for one unit of the non-dimensional time. When interpreting the results a realistic value is given to one unit of the non-dimensional time. For example if one unit of the non-dimensional time is one year then the velocity of 5 cm, specified for the model, means 5 cm/year.

At each time the displacements of the blocks are defined so that the structure is in a quasistatic equilibrium, and all displacements are supposed to be infinitely small, compared with the block size. Therefore the geometry of the block structure does not change during the simulation and the structure does not move as a whole.

2.3 Interaction between the Blocks and the Underlying Medium

The elastic force, which is due to the relative displacement of the block and the underlying medium, at some point of the block bottom, is assumed to be proportional to the difference between the total relative displacement vector and the vector of slippage (inelastic displacement) at the point.

The elastic force per unit area $\mathbf{f}^u = (f_x^u, f_y^u)$ applied to the point with co-ordinates (X, Y) , at some time t , is defined by

$$\begin{aligned} f_x^u &= K_u(x - x_u - (Y - Y_c)(\varphi - \varphi_u) - x_a), \\ f_y^u &= K_u(y - y_u + (X - X_c)(\varphi - \varphi_u) - y_a) \end{aligned} \quad (1)$$

where X_c and Y_c are the co-ordinates of the geometrical center of the block bottom; (x_u, y_u) and φ_u are the translation vector and the angle of rotation (following the general convention, the positive direction of rotation is anticlockwise), around the geometrical center of the block bottom, for the underlying medium at time t ; (x, y) and φ are the translation vector of the block and the angle of its rotation around the geometrical center of its bottom at time t ; (x_a, y_a) is the inelastic displacement vector at the point (X, Y) at time t .

The evolution of the inelastic displacement at the point (X, Y) is described by the equations

$$\frac{dx_a}{dt} = W_u f_x^u, \quad \frac{dy_a}{dt} = W_u f_y^u. \quad (2)$$

The coefficients K_u and W_u in (1) and (2) may be different for different blocks.

2.4 Interaction between the Blocks along the Fault Planes

At the time t , in some point (X, Y) of the fault plane separating the blocks numbered i and j (the block numbered i is on the left and that numbered j is on the right of the fault) the components Δx , Δy of the relative displacement of the blocks are defined by

$$\begin{aligned}\Delta x &= x_i - x_j - (Y - Y_c^i)\varphi_i + (Y - Y_c^j)\varphi_j, \\ \Delta y &= y_i - y_j + (X - X_c^i)\varphi_i - (X - X_c^j)\varphi_j\end{aligned}\quad (3)$$

where X_c^i , Y_c^i , X_c^j , Y_c^j are the co-ordinates of the geometrical centers of the block bottoms, (x_i, y_i) , and (x_j, y_j) are the translation vectors of the blocks, and φ_i , φ_j are the angles of rotation of the blocks around the geometrical centers of their bottoms, at time t .

In accordance with the assumption that the relative block displacements take place only along the fault planes, the displacements along the fault plane are connected with the horizontal relative displacement by

$$\begin{aligned}\Delta_t &= e_x \Delta x + e_y \Delta y, \\ \Delta_l &= \Delta_n / \cos \alpha, \quad \Delta_n = e_x \Delta y - e_y \Delta x.\end{aligned}\quad (4)$$

Here Δ_t and Δ_l are the displacements along the fault plane parallel (Δ_t) and normal (Δ_l) to the fault line on the upper plane; (e_x, e_y) is the unit vector along the fault line on the upper plane; α is the dip angle of the fault plane; and Δ_n is the horizontal displacement, normal to the fault line on the upper plane. It follows from (4) that Δ_n is the projection of Δ_l on the horizontal plane (Fig. 2a).

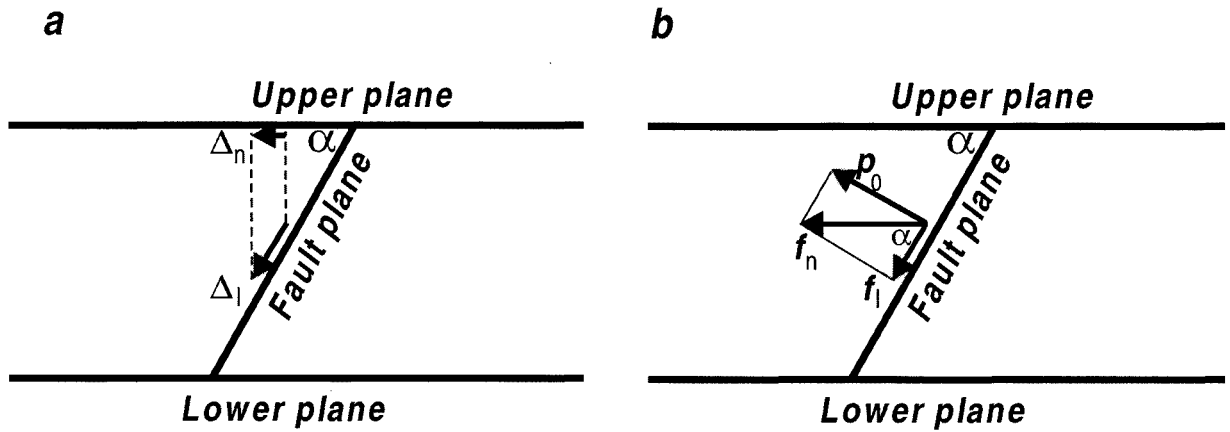


FIGURE 2 Vertical section of a block structure orthogonal to a fault. Relative displacements of blocks Δ_n and Δ_l (a) and forces p_0 , f_l , and f_n (b).

The elastic force per unit area $\mathbf{f} = (f_t, f_l)$ acting along the fault plane at the point (X, Y) is defined by

$$\begin{aligned}f_t &= K(\Delta_t - \delta_t), \\ f_l &= K(\Delta_l - \delta_l).\end{aligned}\quad (5)$$

Here δ_t , δ_l are inelastic displacements along the fault plane at the point (X,Y) at time t , parallel (δ_t) and normal (δ_l) to the fault line on the upper plane.

The evolution of the inelastic displacement at the point (X,Y) is described by the equations

$$\frac{d\delta_t}{dt} = Wf_t, \quad \frac{d\delta_l}{dt} = Wf_l. \quad (6)$$

The coefficients K and W in (5) and (6) may be different for different faults. The coefficient K can be considered as the shear modulus of the fault plane.

In addition to the elastic force, there is the reaction force which is normal to the fault plane; the work done by this force is zero, because all relative movements are tangent to the fault plane. The elastic energy per unit area at the point (X,Y) is equal to

$$e = (f_t(\Delta_t - \delta_t) + f_l(\Delta_l - \delta_l))/2. \quad (7)$$

From (4) and (7) the horizontal component of the elastic force per unit area, normal to the fault line on the upper plane, f_n can be written as:

$$f_n = \frac{\partial e}{\partial \Delta_n} = \frac{f_l}{\cos \alpha}. \quad (8)$$

It follows from (8) that the total force acting at the point of the fault plane is horizontal if there is a reaction force, which is normal to the fault plane (Fig. 2b). The reaction force per unit area is equal to

$$p_0 = f_l \tan \alpha. \quad (9)$$

The reaction force (9) is introduced and therefore there are not vertical components of forces acting on the blocks and there are not vertical displacements of blocks.

Formulas (3) are also valid for boundary faults. In this case one of blocks separated by the fault is a boundary block. The movement of blocks is prescribed by their translation and rotation around the origin of co-ordinates. Therefore the co-ordinates of the geometrical center of the block bottom in (3) are set to zero for any boundary block. For example, if the block numbered j is a boundary block, then $X_c^j = Y_c^j = 0$ in (3).

2.5 Equilibrium Equations

The components of the translation vectors of the blocks and the angles of their rotation around the geometrical centers of the bottoms are found from the condition that the total force and the total moment of forces acting on each block are equal to zero. This is the condition of quasi-static equilibrium of the system and the condition of minimum energy at the same time. The forces arising from the specified movements of the underlying medium and of the boundaries of the block structure are considered only in the equilibrium equations. In fact it is assumed that the action of all other forces (gravity, etc.) on the block structure is balanced and does not cause displacements of the blocks.

In accordance with formulas (1), (3-5), (8), and (9) the dependence of the forces, acting on the blocks, on the translation vectors of the blocks and the angles of their rotations is linear. Therefore the system of equations which describes the equilibrium is linear one and has the following form

$$Az = b \quad (10)$$

where the components of the unknown vector $\mathbf{z} = (z_1, z_2, \dots, z_{3n})$ are the components of the translation vectors of the blocks and the angles of their rotation around the geometrical centers of the bottoms (n is the number of blocks), i.e. $z_{3m-2} = x_m$, $z_{3m-1} = y_m$, $z_{3m} = \varphi_m$ (m is the number of the block, $m = 1, 2, \dots, n$).

The matrix \mathbf{A} does not depend on time and its elements are defined from formulas (1), (3-5), (8), and (9). The moment of the forces acting on a block is calculated relative to the geometrical center of its bottom. The expressions for the elements of the matrix \mathbf{A} contain integrals over the surfaces of the fault segments and of the block bottoms. Each integral is replaced by a finite sum, in accordance with the space discretization described in Section 2.6.

The components of the vector \mathbf{b} are defined from formulas (1), (3-5), (8), and (9) as well. They depend on time, explicitly, because of the movements of the underlying medium and of the block structure boundaries and, implicitly, because of the inelastic displacements.

2.6 Discretization

Time is discretized with a step Δt . The state of the block structure is considered at discrete values of time $t_i = t_0 + i\Delta t$ ($i = 1, 2, \dots$), where t_0 is the initial time. The transition from the state at t_i to the state at t_{i+1} is made as follows:

- (i) new values of the inelastic displacements $x_a, y_a, \delta_t, \delta_l$ are calculated from equations (2) and (6);
- (ii) the translation vectors and the rotation angles at t_{i+1} are calculated for the boundary blocks and the underlying medium;
- (iii) the components of \mathbf{b} in equations (10) are calculated, and these equations are used to define the translation vectors and the angles of rotation for the blocks.

Since the elements of \mathbf{A} in (10) are not functions of time, the matrix \mathbf{A} and the associated inverse matrix can be calculated only once, at the beginning of the calculation.

Formulas (1-9) describe the forces, the relative displacements, and the inelastic displacements at points of the fault segments and of the block bottoms. Therefore the discretization of these surfaces is required for the numerical simulation. The space discretization is defined by the parameter ε , and it is applied to the surfaces of the fault segments and to the block bottoms. The discretization of a fault segment is performed as follows. Each fault segment is a trapezium with bases a and b and height $h = H/\sin\alpha$, where H is the thickness of the layer, and α is the dip angle of the fault plane. The values

$$n_1 = \text{ENTIRE}(h/\varepsilon) + 1, \text{ and } n_2 = \text{ENTIRE}(\max(a,b)/\varepsilon) + 1,$$

are defined, and the trapezium is divided into $n_1 n_2$ small trapeziums by two groups of segments inside it: $n_1 - 1$ segments, parallel to the trapezium bases and spaced at intervals h/n_1 , and $n_2 - 1$ segments connecting the points spaced by intervals of a/n_2 and b/n_2 , respectively, on the two bases. The small trapeziums obtained in such a way are called "cells". The co-ordinates X, Y in (3) and the inelastic displacements δ_t, δ_l in (5) are supposed to be the same for all the points of a cell. These values of the co-ordinates and the inelastic displacements are considered as the average values over the cell. When introduced in formulas (3-5), (8), and (9) they yield the average over the cell of the elastic and reaction forces per unit area. The forces acting on the cell are obtained by multiplying the average forces per unit area by the area of the cell.

The bottom of a block is a polygon. Before discretization it is divided into trapeziums (triangles) by segments passing through its vertices and parallel to the Y axis. The discretization of these trapeziums (triangles) is performed in the same way as in the case of the fault segments. The small trapeziums (triangles) are also called "cells". For all the points of a cell the co-ordinates X, Y and the inelastic displacements x_a, y_a in (1) are assumed to be the same.

2.7 Earthquake and Creep

Let us introduce the quantity

$$\kappa = \frac{|\mathbf{f}|}{P - p_0} \quad (11)$$

where $\mathbf{f} = (f_t, f_l)$ is the vector of the elastic force per unit area given by (5), P is assumed equal for all the faults and can be interpreted as the difference between the lithostatic and the hydrostatic pressure, p_0 , given by (9), is the reaction force per unit area.

For each fault the following three values of κ are considered

$$B > H_f \geq H_s.$$

Let us assume that the initial conditions for the numerical simulation of block structure dynamics satisfy the inequality $\kappa < B$ for all the cells of the fault segments. If, at some time t_i , the value of κ in any cell of a fault segment reaches the level B , a failure ("earthquake") occurs. The failure is meant as slippage during which the inelastic displacements δ_t, δ_l in the cell change abruptly to reduce the value of κ to the level H_f . Thus, the earthquakes occur in accordance with the dry friction model.

The new values of the inelastic displacements in the cell are calculated from

$$\delta_t^e = \delta_t + \gamma f_t, \quad \delta_l^e = \delta_l + \gamma f_l \quad (12)$$

where $\delta_t, \delta_l, f_t, f_l$ are the inelastic displacements and the components of the elastic force vector per unit area just before the failure. The coefficient γ is given by

$$\gamma = 1/K - PH_f / (K(|\mathbf{f}| + H_f \tan \alpha)). \quad (13)$$

It follows from (5), (9), and (11-13) that on obtaining the new values of the inelastic displacements the value of κ in the cell becomes equal to H_f .

After calculating the new values of the inelastic displacements for all the failed cells, the new components of the vector \mathbf{b} are calculated, and from the system of equations (10) the translation vectors and the angles of rotation for the blocks are found. If for some cell(s) of the fault segments $\kappa > B$, the procedure given above is repeated for this cell (or cells). Otherwise the state of the block structure at the time t_{i+1} is determined as follows: the translation vectors, the rotation angles (at t_{i+1}) for the boundary blocks and for the underlying medium, and the components of \mathbf{b} in equations (10) are calculated, and then equations (10) are solved.

The cells of the same fault plane where failure occurs at the same time form a single earthquake. The parameters of the earthquake are defined as follows:

- (i) the origin time is t_i ;
- (ii) the epicentral co-ordinates and the source depth are the weighted sums of the co-ordinates and depths of the cells included in the earthquake (the weight of each cell is given by its square divided by the sum of squares of all the cells included in the earthquake);
- (iii) the magnitude is calculated from

$$M = 0.98 \lg S + 3.93, \quad (14)$$

where S is the sum of the squares of the cells (in km^2) included in the earthquake and the values of coefficients are specified in accordance with Utsu and Seki (1954).

It is assumed that the cells, in which a failure has occurred, are in the creep state immediately after the earthquake. It means that the parameter W_s ($W_s > W$) is used instead of W for these cells in (6) describing the evolution of inelastic displacements; W_s may be different for different fault planes. After each earthquake a cell is in the creep state as long as $\kappa > H_s$, whereas when $\kappa \leq H_s$, the cell returns to the normal state and henceforth the parameter W is used in (6) for this cell.

2.8 Hierarchy of Faults

Fault features can be taken into consideration through the values of the constants K , W , W_s and the levels B , H_f , H_s .

The hierarchy of faults is controlled by the hierarchy of structures separated by them. Larger faults separate larger structures. Note that accordingly to the fault definition the larger fault does not mean the longer fault.

It seems natural that the same value of elastic displacement leads to a smaller elastic force for the larger fault than for a smaller one. Thus the value of K has to be smaller for a larger fault.

Larger faults separating larger structures are usually the more strongly fractured and less consolidated zones than smaller faults, and the same force can lead to larger slippage (inelastic displacement) for a larger fault than for a smaller one. Thus the values of W and W_s have to be larger for larger faults than for smaller ones.

The more strongly fracturing of the larger faults can be a cause that earthquakes occur in the larger faults for smaller values of the parameter κ than in the smaller ones. This can be reflected in smaller values of the levels B , H_f , H_s for the larger faults than for the smaller ones.

The qualitative arguments given above can be used as some indications for selecting the values of constants K , W , W_s and levels B , H_f , H_s if the fault hierarchy is known.

III. MODELLING OF LITHOSPHERE BLOCK DYNAMICS AND SEISMICITY

3.1 Dependence of Synthetic Seismicity on Structure Fragmentation and Boundary Movements

The model was applied to study the dependence of features of the synthetic earthquake flow on the structure fragmentation and the boundary movement (Keilis-Borok et al. 1997). Three groups of block structures with increasing structure fragmentation inside each group were considered. The respective schemes of faults of these structures on the upper plane are shown in Fig. 3. One structure (BS1) belongs to all groups. Two other structures of the first (BS12, BS13), the second (BS22, BS23), and the third (BS32, BS33) group are obtained from BS1 by self-similar subdivision (Bariere and Turcotte 1994).

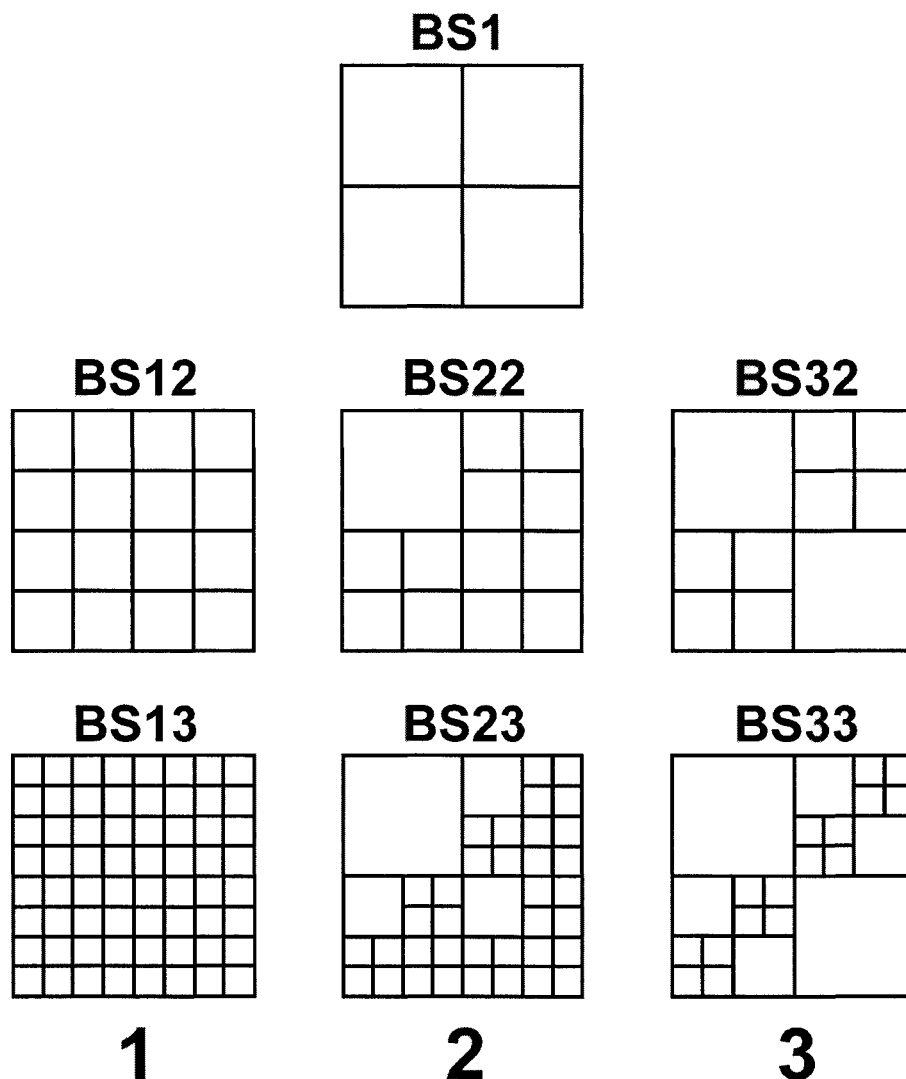


FIGURE 3 Faults on the upper plane from block structures under consideration: (1) the first group (BS1, BS12, BS13); (2) the second group (BS1, BS22, BS23); and (3) the third group (BS1, BS32, BS33).

Two types of boundary movement are considered (Fig. 4). The first type is the progressive movement of the boundaries with the same velocity as shown in Fig. 4a. The second type includes the progressive movement and the rotation of the boundaries as shown in Fig. 4b. The underlying medium under all the blocks of the structures does not move.

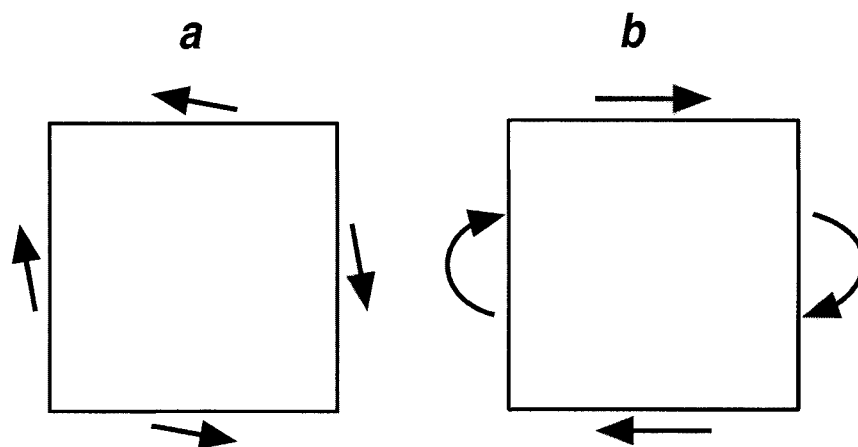


FIGURE 4 Types of boundary movements considered. The arrows stand for the velocity vectors of the boundaries: (a) the first type (without rotation), the angle between the velocity vectors and the respective boundary faults is 10° ; (b) the second type (with rotation).

The synthetic seismicity obtained by modeling is characterized by several features including the FM relation (the Gutenberg-Richter curve). The cumulative FM plots for the synthetic catalogs are presented in Figs 5 and 6. These plots are in accordance with the FM relation for the observed seismicity: the logarithm of the number of earthquakes depends linearly on the magnitude.

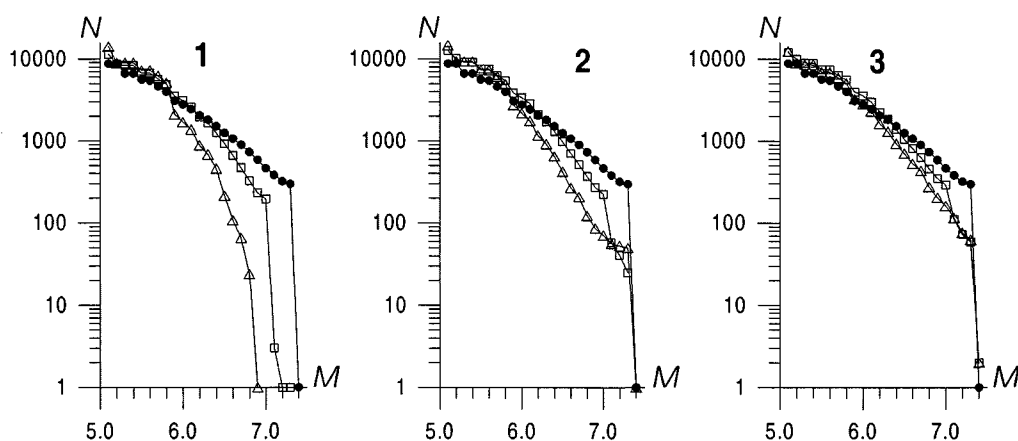


FIGURE 5 Cumulative frequency-magnitude plots for synthetic catalogs obtained for the boundary movement without rotation from 3 groups of structures: (1) first, (2) second, and (3) third. Curves are marked as follows: dots (obtained from BS1), squares (BS12, BS22, and BS32), and triangles (BS13, BS23, and BS33).

Fig. 5 shows that in case of the boundary movement without rotation the slope of the FM plot increases when structure fragmentation increases in each group. When the boundary movement with rotation is considered (Fig. 6) changing of the FM plot is *antipodal*: the slope of the plot decreases when structure fragmentation increases in each group.

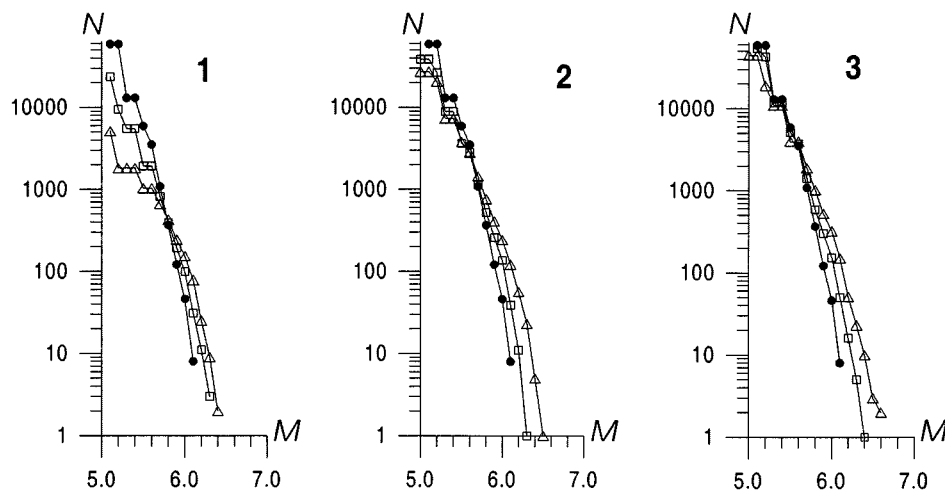


FIGURE 6 Cumulative frequency-magnitude plots for synthetic catalogs obtained for the boundary movement with rotation. Notations are the same as in Fig. 5.

These results show that the features of a synthetic earthquake flow depend on the geometry of the block structure and on the boundary movement. The character of the dependence on the geometry alters principally when the boundary movement of another type is specified. Note that for the boundary movement with rotation the dependence of the considered characteristics of the seismic flow on the structure fragmentation is in contradiction with the agreed-upon opinion.

3.2 Space-temporal Correlation between Synthetic Earthquakes

The block model was studied to look for space-temporal correlation between synthetic earthquakes (Gorshkov et al. 1997; Rotwain and Soloviev 1998; Maksimov and Soloviev 1999; Soloviev and Vorobieva 1999; Vorobieva and Soloviev 2001).

The possibility of earthquakes *clustering* in the synthetic catalog was considered by Maksimov and Soloviev (1999). It is of vital importance to determine whether clustering is caused by specific tectonic features of a region or is a general phenomenon for a wide variety of neotectonic conditions which reflects general features of systems of interacting blocks of the seismogenic lithosphere. The results obtained show that the phenomenon of clustering is observed for a structure consisting of four identical square blocks when a simple movement of one boundary is prescribed, and this clustering of earthquakes in a synthetic catalog arising from modeling of dynamics of a simple block structure is in favor of the second hypothesis.

The geometry of this block structure is shown in Fig. 7 as schemes of faults on the upper plane. It is assumed that the boundary consisting of the fault segments numbered 8 and 7 moves translationally along X axis and rotates around the common point of segments 8 and 7 on the upper plane (as shown in Fig. 7). The other parts of the structure boundary and the underlying medium do not move.

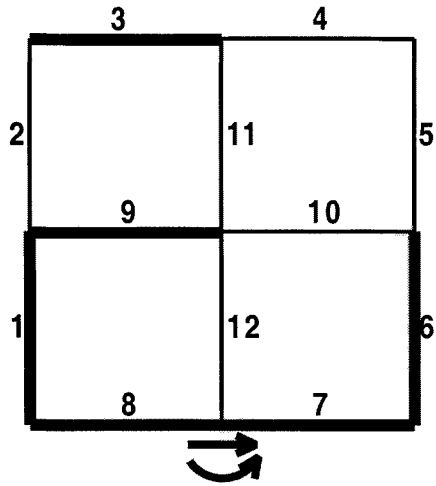


FIGURE 7 Configuration (on the upper plane) of faults of the block structure, for which clustering of synthetic earthquakes and long-range interaction between them were studied. The movement specified for the boundary consisting of the fault segments numbered 7 and 8 is shown below.

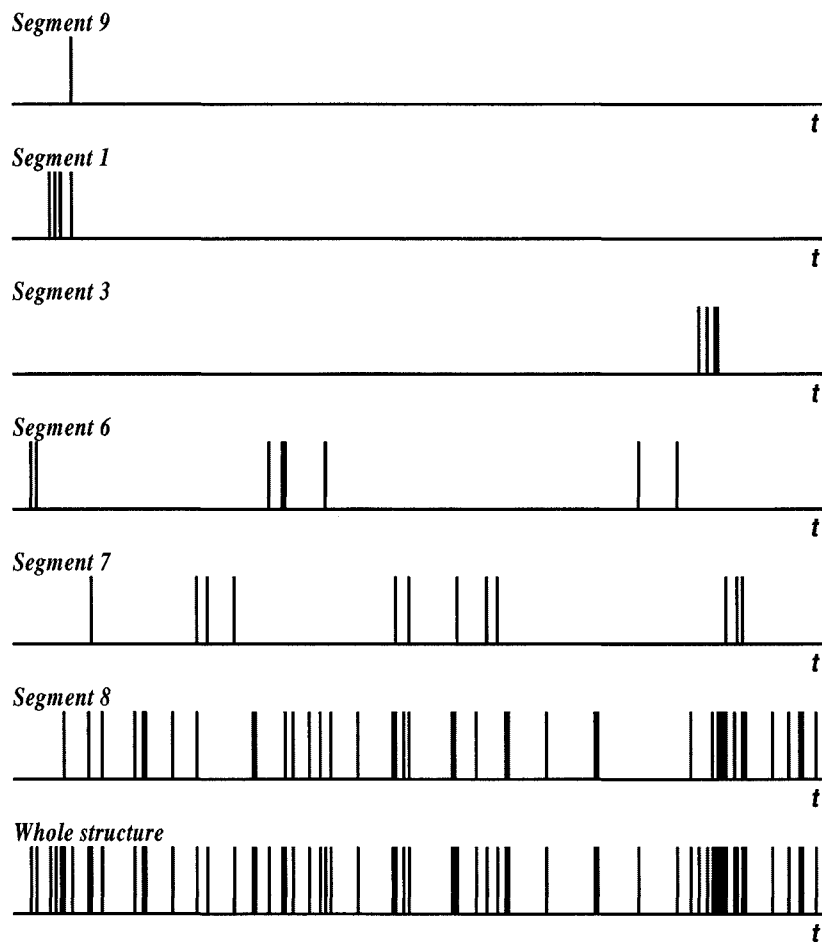


FIGURE 8 Clustering of synthetic earthquakes. The moments of the earthquakes (vertical lines) for individual fault segments (numbered as in Fig. 7) and for the whole structure for the time interval of 3 units.

The occurrence times of synthetic earthquakes (vertical lines) are shown in Fig. 8 for individual fault segments and for the whole structure for the time interval of 3 units. Earthquakes occur on six fault segments. These segments are marked in Fig. 7 by thick lines. The segment 9 has one earthquake only for the period under consideration. Clustering of earthquakes appears clearly on the fault segments 1, 3, 6, and 7. The segment 8 has the largest number of earthquakes. Here the clustering appears weaker: the groups of earthquakes are diffuse along the time axis. The pattern for the whole structure looks like as for segment 8, and groups of earthquakes can be also identified. Clustering of earthquakes for other time intervals is not substantially different from that presented in Fig. 8.

The clustering of earthquakes found in the model gives opportunity to use modeling to study the phenomenon of clustering of earthquakes in the specific seismoactive regions. In particular dependence of clustering on geometry of a block structure and values of parameters of the model can be ascertained.

The block structure presented in Fig. 7 was also considered to study *long-range interaction* between synthetic events (Soloviev and Vorobieva 1999; Vorobieva and Soloviev 2001). Numerical experiments show that there is the long-range interaction between synthetic earthquakes. This is detected by the statistical analysis of the synthetic earthquake catalogs obtained. At the same time increasing the strength level for individual faults to prevent earthquake occurrence on them affect pronouncedly earthquake flows on other faults. This means that the long-range interaction found in the observed seismicity (e.g. Benioff 1951; Duda 1965; Prozorov 1991, 1993; Press and Allen 1995) could be explained by considering lithosphere blocks being perfectly rigid in comparison with fault zones, separating them, and the underlying medium.

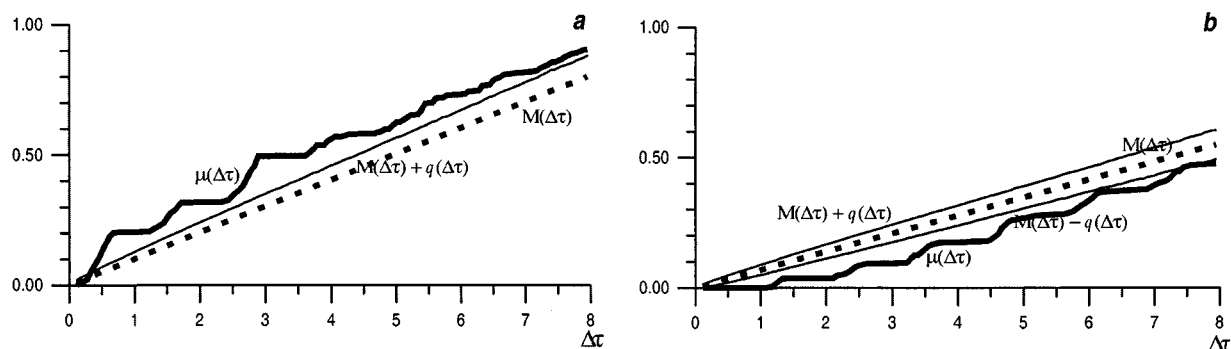


FIGURE 9 Functions $\mu(\Delta\tau)$, $M(\Delta\tau)$, $M(\Delta\tau) \pm q(\Delta\tau)$ showing that strong ($M \geq 6.6$) earthquakes occur often in fault segments 7&8 after strong ($M \geq 6.0$) earthquakes of fault segment 9 (a) and that strong earthquakes occur seldom in fault segment 9 after strong earthquakes of fault segments 7&8 (b).

Specifically the long-range interaction was found in the model under consideration (Fig. 7) for the earthquakes with magnitude $M \geq 6.6$, occurred in the fault plane (F_2) containing segments 7 and 8, and the earthquakes with $M \geq 6.0$, occurred in fault segment 9 (F_1). Namely the earthquakes of F_2 occur more frequent after the earthquakes of F_1 than on the average for the whole interval of simulation. Fig. 9a shows the plots of functions $\mu(\Delta\tau)$, $M(\Delta\tau)$, which are average numbers of the earthquakes of F_2 occurred during time intervals $\Delta\tau$ after the earthquakes of F_1 and during arbitrary time intervals $\Delta\tau$ respectively. Fig. 9a shows also the plot of the function $M(\Delta\tau) + q(\Delta\tau)$ where $q(\Delta\tau)$ is the standard deviation of $\mu(\Delta\tau)$ when random occurrence times of the earthquakes of F_1 are considered. One can see that

while $0.5 < \Delta\tau < 7.0$ the difference between $\mu(\Delta\tau)$ and $M(\Delta\tau)$ exceeds appreciably $q(\Delta\tau)$. For instance, $\mu(3.0) = 0.495$, $M(3.0) = 0.303$, and $q(3.0) = 0.047$, and therefore the difference $\mu(3.0) - M(3.0) = 0.192$ exceeds $q(3.0)$ more than in 4 times.

A question arises whether the phenomenon found reflects the joint clustering of the strong earthquakes occurred in segments 7, 8, and 9. To answer on this question it has been checked whether the earthquakes with $M \geq 6.0$, occurred in segment 9, succeed the earthquakes with $M \geq 6.6$, occurred in the fault plane containing segments 7 and 8. In other words the moments of the strong earthquakes in F_1 and F_2 are replaced with each other in the analysis given above. The obtained functions $\mu(\Delta\tau)$, $M(\Delta\tau)$, $M(\Delta\tau) + q(\Delta\tau)$, and $\lambda(\Delta\tau)$ and are shown in Fig. 9b. In this case in the interval $0.5 < \Delta\tau < 7.0$ the function $\mu(\Delta\tau)$ does not exceeds $M(\Delta\tau)$ and even is less than function $M(\Delta\tau) - q(\Delta\tau)$, which is also shown in Fig. 9b. For instance, $\mu(3.0) = 0.094$, $M(3.0) = 0.208$, and $q(3.0) = 0.033$, and therefore the difference $M(3.0) - \mu(3.0) = 0.114$ exceeds $q(3.0)$ more than in 3 times. It means that the strong earthquakes of F_1 occur more seldom after the strong earthquakes of F_2 than on the average for the whole interval of simulation.

3.3 Study of Seismicity of Arc Subduction Zones

Seismicity in many most active regions of the world is caused by interaction of continents with oceanic plates along subduction zones. Features of earthquake flow differ in different segments of these zones and the origin of this difference is not yet clear. It is natural to suggest that these differences are associated, among other factors, with a dip angle of subduction zone and with direction of relative movement of continental and oceanic plates. Dynamics of a block structure approximating an arc subduction zone, which is typical for regions of island arcs, was modeled by Rundquist and Soloviev (1999) to single out the impact of single factors on the synthetic seismicity. This modeling was carried out with various dip angles of the subduction zone and various directions of motion of “a continent” and “an oceanic plate”. Distributions of earthquake epicenters and other characteristics of the synthetic earthquake flow obtained were studied.

Basic relations, which are common for different subduction zones, were looked for in this study. Accordingly, a simplified structure, not imitating a specific subduction zone has been considered. It consists of one arched block A , which common part with the upper plane is shown in Fig. 10. It is bounded by two horizontal planes separated by a vertical distance $H = 100$ km, comparable to the thickness of the lithosphere. Fault planes intersecting the layer between these horizontal planes form the lateral boundaries of the block A . The fault planes are numbered from 1 to 8 (Fig. 10). Block A is interpreted to be an island arc and the adjoining edge of the continent or the back-arc basin. The subduction zone, where the continent interacts with the oceanic plate, is represented by the system of fault planes numbered 1-5 (Fig. 10), which have the same dip angle α . Faults 6-8 are introduced solely to limit the structure and $K = 0$ was specified for them in formula (3). Therefore any displacements do not produce forces in these fault planes. Movements were specified for the underlying medium and the boundary consisting of fault planes 1-5. The direction of the underlying medium movement coincides with the positive direction of axis X (Fig. 10). The boundary movement, which models the movement of an oceanic plate bordering a continent, has the opposite direction, which is defined by the angle β between the vector of its velocity and the negative direction of axis X (Fig. 10).

As a result of modeling the dependence of the synthetic seismicity, obtained in the abstract model of a subduction zone, on the slope of the zone α and on the angle β between directions, in which the plates, flanking the zone, move is characterized as follows.

1. The seismic activity grows when the slope α is increasing from 30° to 40° - 50° . It decreases slightly with further increasing of α and drops when α exceeds a certain critical

value at about 70° .

2. As a function of the directions' difference β the seismic activity has a peak at about 40° .

3. The slope of FM plot for the synthetic catalogs increases when β increases.

4. Seismicity migrates along the island arc related to the subduction zone. In most cases migration occurs in the same direction as the projection of the oceanic plate velocity on the arc; in some cases it goes in the opposite direction.

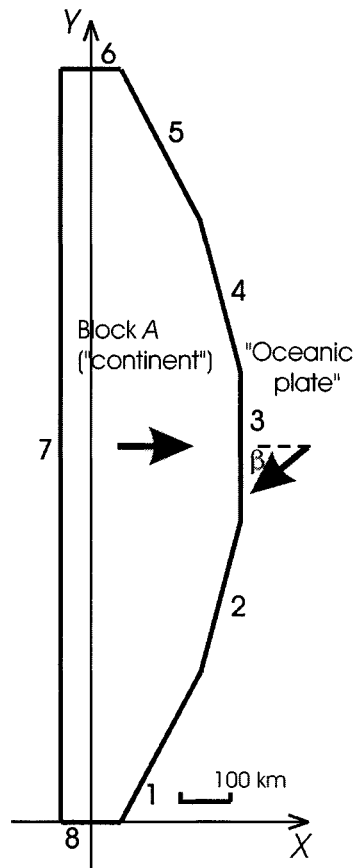


FIGURE 10 Configuration (on the upper plane) of faults of the block structure approximating an arc subduction zone: 1-8 - numbers, identifying the faults; arrows show directions of movement of the medium underlying the block A and of the boundary formed by faults 1-5.

The block structure approximating Sunda Arc (Sunda Isles) was considered by Soloviev et al. (1999b). The dependence of features of the synthetic seismicity on the movements specified was studied for it. Sunda Arc lies on the boundary between Eurasia and Australia plates (Fig. 11). One block is considered to represent a part of Eurasia plate. Its thickness $H = 130$ km. This block is bounded by 7 fault planes numbered from 1 to 7. The corresponding faults on the upper plane are shown in Fig. 11 by solid lines. Fault planes 1-4 have the same dip angle 21° . The dip angles of fault planes 5-7 are 85° , 159° , and 85° correspondingly. The block bottom is shown in Fig. 11 by a dashed line.

Fault planes 1-4 form the boundary zone between Eurasia and Australia plates. The movement of this boundary and the movement of the underlying medium were specified so as to approximate the movement of Australia relative to Eurasia accordingly HS2-NUVEL1 model (Gripp and Gordon 1990). Fault planes 5-7 are introduced to limit the structure and $K =$

0 was specified for them in formula (3).

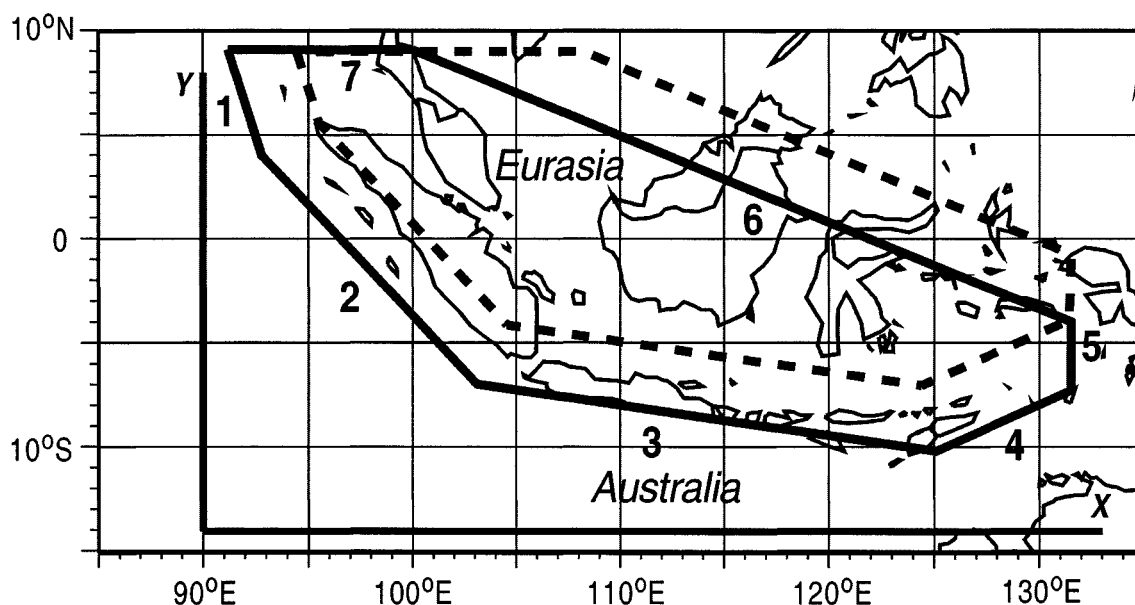


FIGURE 11 Model of Sunda Arc: configuration of the faults on the upper plane (solid lines) and on the lower plane (dashed lines); 1-7 - numbers, identifying the faults.

The observed seismicity of the region is compared with the stable part of the synthetic earthquake catalog for the period corresponding to 100 years. The cumulative FM relations for the synthetic catalog and the observed seismicity are given in Fig. 12. One can see that the slopes of the curves (B -values) are close, but the curve, obtained for the synthetic catalog, is shifted to the larger magnitudes. The value of the shift is about 1. The curve for the synthetic catalog with the magnitudes, reduced by 1, is also given in Fig. 12. This curve is rather close to the one for the observed seismicity. It was also found that the synthetic seismicity has other common features with the observed one: location of the largest events, direction of migration of the earthquakes.

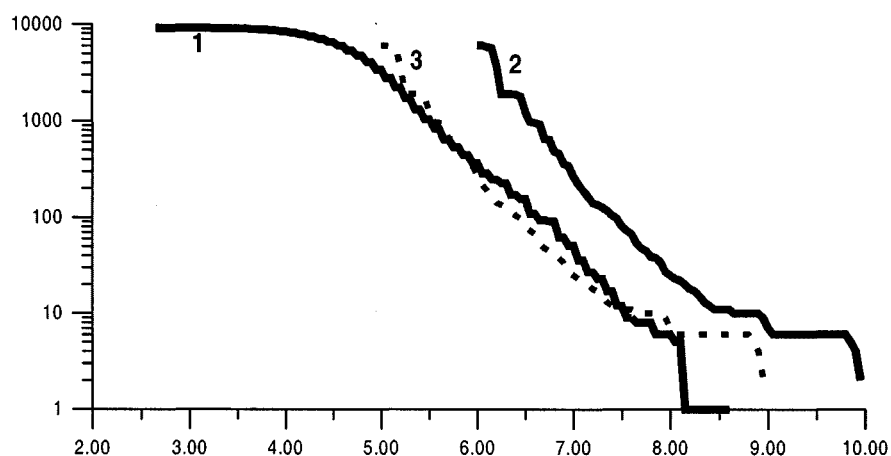


FIGURE 12 Cumulative FM plots for the observed seismicity of Sunda Arc (1), for the synthetic catalog (2), and for the synthetic catalog with the magnitude reduced by 1 (3).

Several experiments have been made to study dependence of the cumulative Gutenberg-Richter curve for the synthetic earthquake catalog on the movements specified in the model. In the first group of the experiments the angle velocity of the boundary, formed by faults 1-4, was varied and its translation velocity was the same as in the basic variant. It was found that if the angle velocity is significantly smaller than in the basic variant then B -value of the Gutenberg-Richter curve is smaller also. The larger B -value is obtained for the larger angle velocity. This conforms to the results obtained by Keilis-Borok et al. (1997). In the second group of the experiments the direction of the vector of the translation velocity of the boundary varied and its angle velocity was the same as in the basic variant. It was found that B -value of the Gutenberg-Richter curve depends on the direction of the vector of the translation velocity of the boundary. Therefore variation of the movements, specified in the model, changes B -value obtained for the synthetic seismicity.

3.4 Models of Block-and-fault Dynamic of the Specific Seismoactive Regions

A geometry of real faults and blocks was considered in block models of *the Vrancea earthquake-prone region* in Romania (Panza et al. 1997). The numerical experiments gave the values of the model parameters supplying synthetic earthquake catalogs with the spatial distribution of epicenters and hypocenters close to that observed in the Vrancea region. FM relations obtained for the synthetic and real catalogs had common features. The source mechanism of the synthetic earthquakes was also considered (Soloviev et al. 2000). Strike and dip define the azimuth and the dip angle of the rupture plane, while the slip defines the direction of the displacement in the rupture plane. Therefore, in the model, strike and dip are prescribed by the block structure geometry and do not depend on the variation of the model parameters. Thus, for the synthetic earthquakes, only the dependence of the slip on the variation of the model parameters was studied, and a comparison was made with observations. An effect of a sinking relic slab beneath Vrancea on the intermediate-depth seismicity was studied by Ismail-Zadeh et al. (1999).

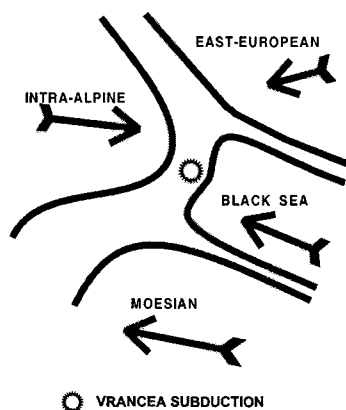


FIGURE 13 Gross kinematic model proposed for the double subduction process in the Vrancea region (modified after Mocanu 1993).

In accordance with Arinei (1974) the main structural elements of the Vrancea region are: (i) the East-European plate; (ii) the Moesian, (iii) the Black Sea, and (iv) the Intra-Alpine (Pannonian-Carpathian) subplates (Fig. 13). The fault separating the East-European plate from the Intra-Alpine and Black Sea subplates and the fault separating the Intra-Alpine and Black Sea subplates have the dip angle significantly different from 90° (Mocanu 1993). The

main directions of the movement of the various plates are shown in Fig. 13. This information is sufficient to define the block structure, which can be considered as a rough approximation of the Vrancea region, and the movements, which can be used for the numerical simulation of the dynamics of this block structure.

The configuration of the faults on the upper plane of the block structure used to model the Vrancea region is presented in Fig. 14. The thickness of the layer is $H = 200$ km, which corresponds the depth of the deeper earthquakes in the Vrancea region. The movement of the underlying medium and the movement of the boundary, which consists of the fault planes 2 and 3, are specified to be progressive. They are shown in Fig. 14 by solid arrows. The boundary fault planes 1, 4, and 5 do not correspond to any real geological structure of the Vrancea region and are introduced only to limit the block structure. These faults do not move and $K = 0$ was specified for them in formula (3).

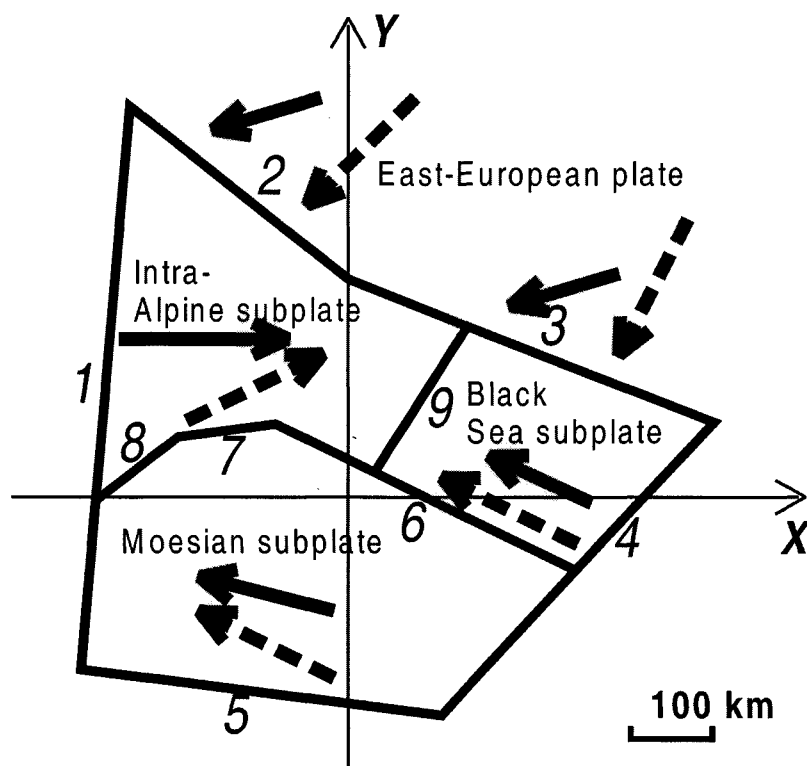


FIGURE 14 The block structure used in the numerical simulation; the numbers of the faults (1 - 9) are indicated. The arrows outside the block structure indicate the movement of boundary blocks while those inside the block structure indicate the movement of the underlying medium. Solid arrows show the velocities specified in the basic variant. Dashed arrows show the velocities specified in the experiment on changing the movements.

The observed seismicity of the region for the period 1900-1995 is presented in Fig. 15 while the map with the distribution of epicenters contained in the synthetic catalog is given in Fig. 16. Most of the synthetic events including all large ($M > 6.7$) ones occur on fault 9 (the cluster A in Fig. 16). This corresponds to the subduction zone of Vrancea, where most of the observed seismicity including four largest earthquakes of the twentieth century is concentrated (the cluster A in Fig. 15). Some events occur on fault plane 6, and they appear as a cluster of epicenters (cluster B in Fig. 16) located to the south-west of the main seismicity area and separated from it by a non-seismic zone. An analogous cluster of epicenters can be seen on the map of the observed seismicity (cluster B in Fig. 15). The third cluster of events

(cluster *C* in Fig. 16) groups on fault plane 8 and corresponds to the cluster *C* of the observed seismicity in Fig. 15. On the map of the observed seismicity (Fig. 15) there are several additional clusters of epicenters, which are absent in the synthetic catalog. This is not surprising since only few main seismic faults of Vrancea region are included in the model. To obtain a more realistic distribution of the synthetic epicenters requires the use of a block structure containing a more detail description of the real system of faults. Nevertheless the considered very simple structure, consisting of only three blocks, allows us to reproduce the main features of the distribution in space of the real seismicity.

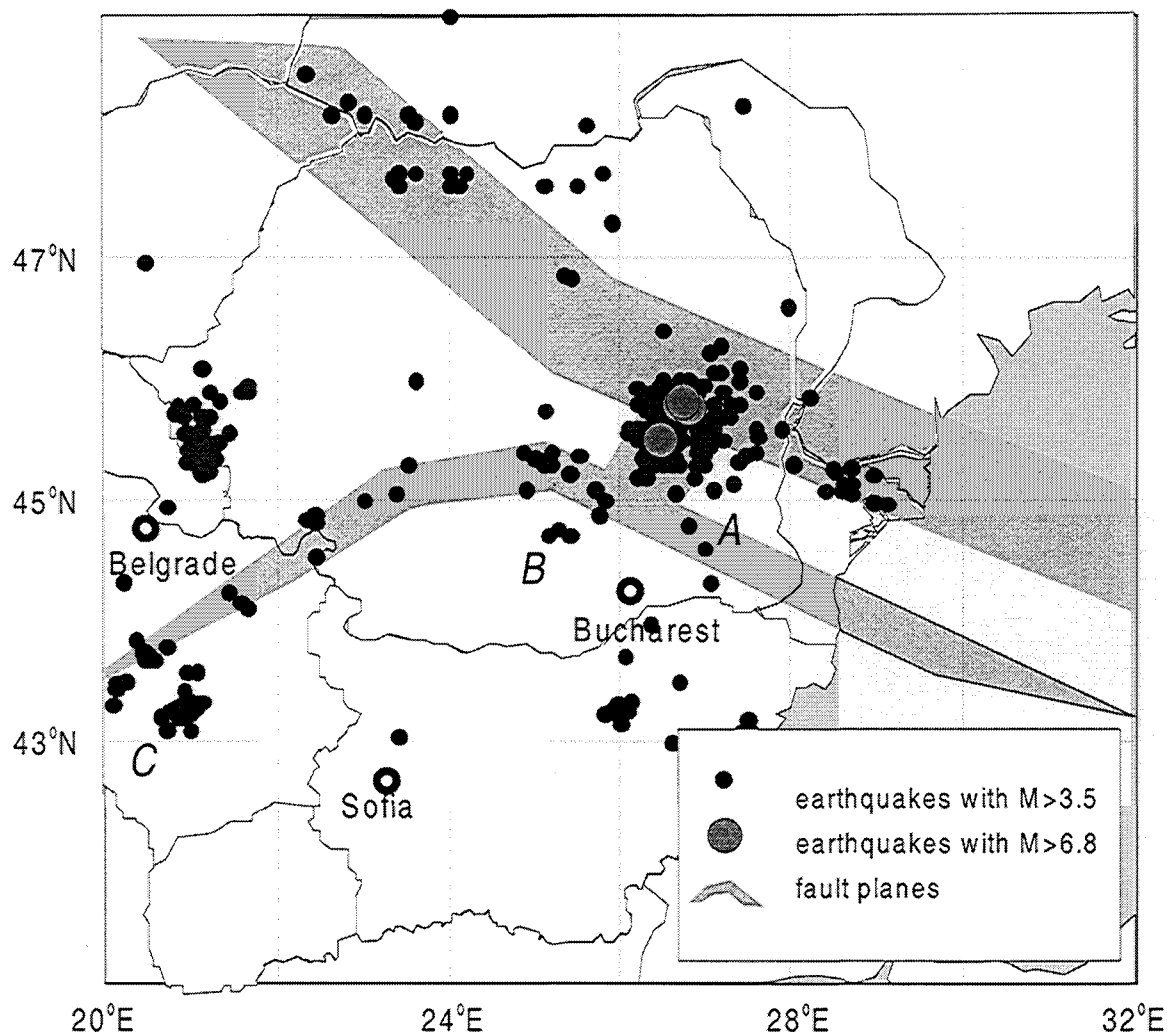


FIGURE 15 Map of the observed seismicity in Vrancea in the period 1900-1995. The grey areas are the projections on the upper plane of the fault planes with $K \neq 0$.

The FM plots for the observed seismicity of Vrancea and for the synthetic catalog are presented in Fig. 17. The curve constructed from the synthetic catalog (dashed line) is almost linear, and it has approximately the same slope as the curve constructed from the observed seismicity (solid line). Using the FM plots and the duration of the real catalog it can be estimated that the synthetic earthquake catalog corresponds to 7000 years.

The various numerical experiments were carried on changing the values of the parameters of the model in order to study the dependence of the synthetic earthquake catalog on values of the model parameters (Soloviev et al. 1999a). An example of changing the space distribution of the epicenters of the synthetic earthquakes when the velocities of the

boundaries and the underlying medium are changed is given in Fig. 18. The velocities specified in this experiment are shown in Fig. 14 by dashed arrows.

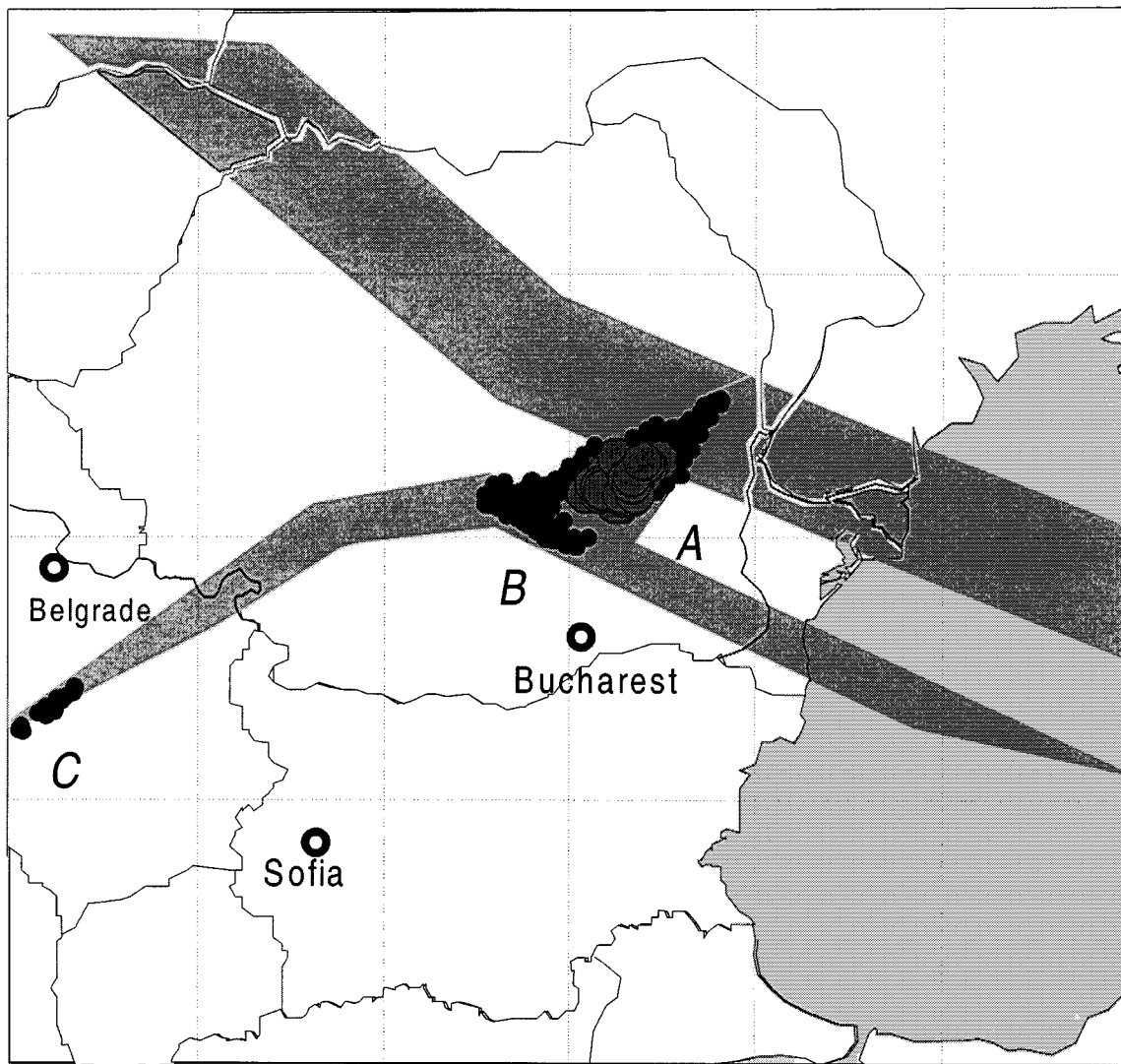


FIGURE 16 Map of the synthetic seismicity, obtained from the simulation of the dynamics of the Vrancea block structure. The grey areas are the projections on the upper plane of the fault zones with $K \neq 0$.

Comparison of the spatial distribution of earthquake epicenters from the synthetic catalogs obtained for various movements of the structure boundary and the underlying medium shows that the spatial distribution depends substantially on the movements specified. The results of the tests indicate the possibility to use the procedure of block structure dynamics modeling to reconstruct the ranges of some parameters used to describe the real regional tectonics. Seismic activity of a fault depends on velocities relative tectonic motions along it, and in a fault system these motions are interconnected. Therefore the spatial distribution of seismicity can be used not only as a characteristic for comparing the activity within different faults, but also for the reconstructing block motions. It is even possible to formulate the inverse problem: To reconstruct the motions of boundary blocks and the underlying medium, which produce driving forces in the model, on the basis of the observed epicenter distribution and of other seismicity features.

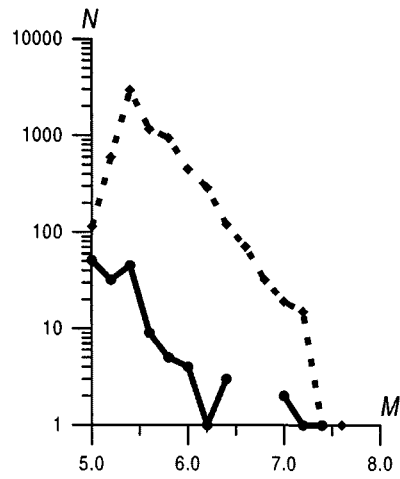


FIGURE 17 FM plots for the observed (solid line) and the synthetic (dashed line) catalogs.

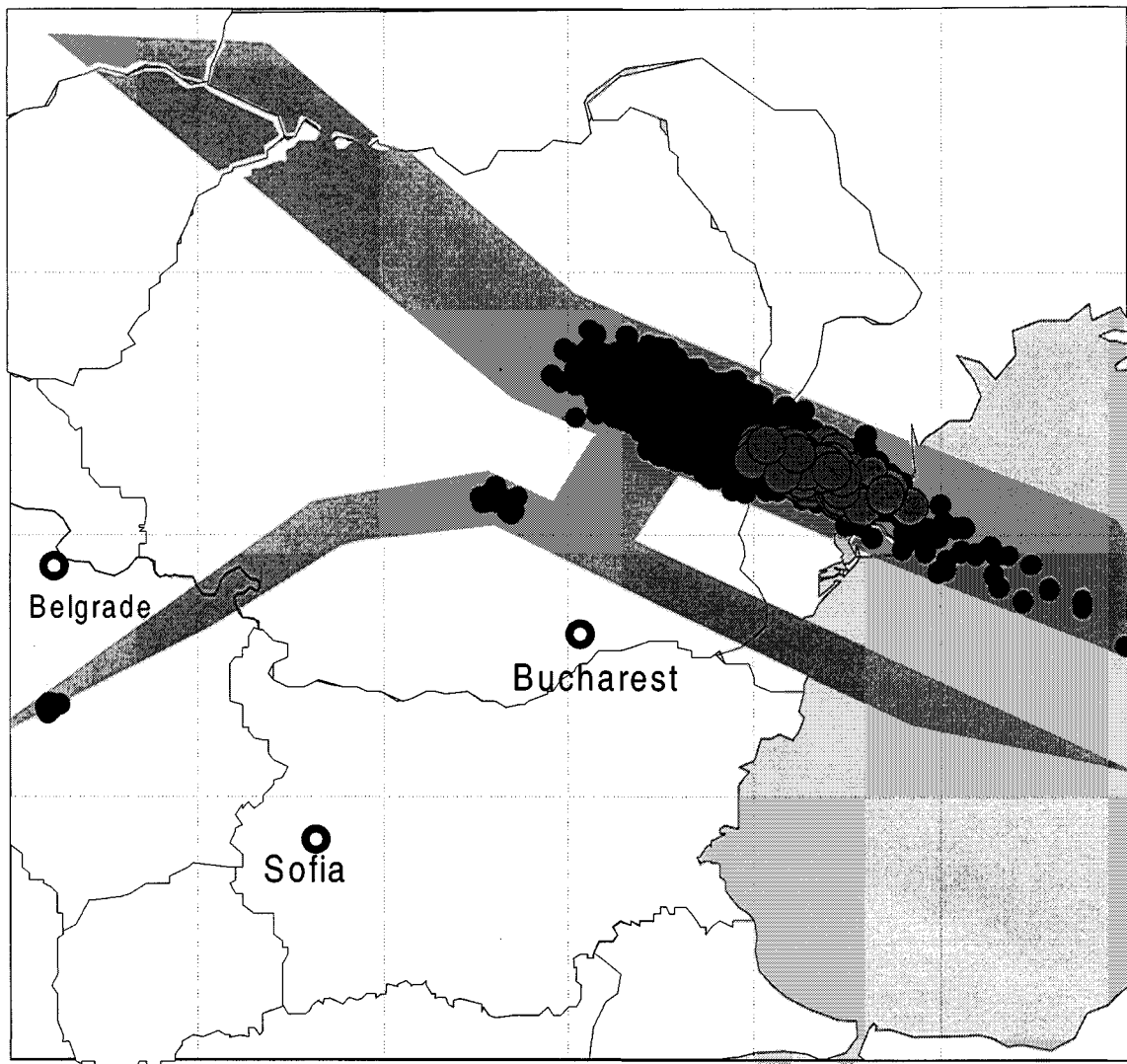


FIGURE 18 Map of the epicenters of the synthetic earthquakes, obtained when the velocities of the structure boundary and the underlying medium were specified as shown in Fig. 14 by dashed arrows. The grey areas are the projections on the upper plane of the fault zones with $K \neq 0$.

The block models of *the Western Alps* (Gabrielov et al. 1994; Gasilov et al. 1995; Gorshkov and Soloviev 1996; Gorshkov et al. 1997; Vorobieva et al. 2000) were developed on the basis of the morphostructural zoning scheme of the region (Cisternas et al. 1985; Vorobieva et al. 2000). The basic principals of the morphostructural zoning are formulated by Alekseevskaya et al. (1977). Several synthetic catalogs of earthquakes for the Western Alps are generated as a result of the numerical simulation. The space distribution of epicenters of the synthetic earthquakes reflects some features of the observed seismicity distribution. There is a similarity of FM relations for the synthetic and observed seismicity. The concentration of the synthetic events is founded out in the model (Gorshkov and Soloviev 1996; Gorshkov et al. 1997; Vorobieva et al. 2000) in the places where no large earthquakes are reported in the catalogs, but which were previously identified as high seismically active by pattern recognition algorithms (Cisternas et al. 1985). The earthquake prediction algorithm M8 (Keilis-Borok and Kossobokov 1990) was applied to the synthetic earthquake catalog obtained in the model (Gabrielov et al. 1994; Gasilov et al. 1995). The result of the application can be considered as satisfactory.

The block model of *the Near East region* was developed and studied by Sobolev et al. (1999).

IV. CONCLUSION

The results obtained show that modeling of block structure dynamics is a useful tool to study relations between geometry of faults and block movements and earthquake flow. This includes premonitory seismicity patterns. It follows from the results of application of earthquake prediction algorithms to the synthetic earthquake catalog (Gabrielov et al. 1990, 1994) that the modeling may be applied to test the existing earthquake prediction algorithms, and to develop new ones.

The following further developments of the model of block structure dynamics may be outlined.

1. Considering in the model 3D movements of blocks. The first results have been already obtained in this direction (Soloviev et al. 1996; Melnikova et al. 1997; Rozenberg and Soloviev 1997).

2. Developing the model, which considers sphericity of the Earth. It may be used for modeling of dynamics of the main tectonic plates in global scale (Digas et al. 1999; Melnikova et al. 2000).

3. Combining the model of block structure dynamics and other models of seismicity, in particular the scaling organization of fracture tectonics (S.O.F.T.) model (Allègre et al. 1995; Narteau et al. 2000). This will describe the short-term process of energy release through earthquakes and depict the dynamics of the fault network separating the blocks by more adequate way than the model of block structure dynamics does.

The model may be applied to study real seismoactive regions such as the Apennines, the Himalayas, California etc. The measure of success is a comparison with the observed seismicity. The values of the parameters of the model, for which the correspondence between the synthetic and the observed catalogs is achieved, may be useful for estimation of the velocities of the tectonic movements and of the values of the physical parameters connected with the dynamic processes taking place in the fault zones. If the relevant segment of the synthetic catalog, which approximates the observed earthquake flow with sufficient accuracy, would be identified, then the part of the synthetic catalog immediately following this segment may be used to predict the future behavior of the seismicity of the region.

Acknowledgements. These studies were partly done at the Abdus Salam International Center for Theoretical Physics, (Trieste, Italy) within the framework of the SAND group activity and supported by a subcontract with Cornell University, Geological Sciences, under EAR-9804859 from the U.S. National Science Foundation and administered by the U.S. Civilian Research & Development Foundation for the Independent States of the Former Soviet Union (CRDF), by International Science and Technology Center (Moscow, project # 1293), by NATO (SFP project 972266), by Russian Foundation for Basic Research (grant # 00-15-98507), and by James S. McDonnell Foundation within the framework of the 21st Century Collaborative Activity Award for Studying Complex Systems (project “*Understanding and Prediction of Critical Transitions in Complex Systems*”).

REFERENCES

- Alekseevskaya, M.A., A.M. Gabrielov, A.D. Gvishiani, I.M. Gelfand, and E.Ya. Ranzman (1977). Formal morphostructural zoning of mountain territories. *J. Geophys.*, **43**: 227-233.
- Allègre, C.J., J.-L. Le Mouél, H.D. Chau, and C. Narteau (1995). Scaling organization of fracture tectonics (SOFT) and earthquake mechanism. *Phys. Earth. Planet. Inter.*, **92**: 215-233.
- Arinei, St. (1974). *The Romanian Territory and Plate Tectonics*. Technical Publishing House, Bucharest (in Romanian).
- Bariere, B., and D.L. Turcotte (1994). Seismicity and self-organized criticality, *Phys. Rev. E*, **49**, 2: 1151-1160.
- Benioff, H. (1951). Global strain accumulation and release as related by great earthquakes. *Bull. Geol. Soc. Amer.*, **62**: 331-338.
- Cisternas, A., P. Godefroy, A. Gvishiani, A.I. Gorshkov, V. Kosobokov, M. Lambert, E. Ranzman, J. Sallantin, H. Saldano, A. Soloviev, and C. Weber (1985). A dual approach to recognition of earthquake prone areas in the western Alps. *Annales Geophysicae*, **3**, 2: 249-270.
- Digas, B.V., V.L. Rozenberg, P.O. Sobolev, and A.A. Soloviev (1999). *Spherical Model of Block Structure Dynamics*. Fifth Workshop on Non-Linear Dynamics and Earthquake Prediction, 4 - 22 October 1999, Trieste, ICTP, H4.SMR/1150-5, 20 pp.
- Duda, S.J. (1965). Secular seismic energy release in the circum Pacific belt. *Tectonophysics*, **2**, 5: 409-452.
- Gabrielov, A.M., V.I. Keilis-Borok, T.A. Levshina, and V.A. Shaposhnikov (1986). Block model of dynamics of the lithosphere. In V.I. Keilis-Borok and A.L. Levshin (eds), *Mathematical Methods in Seismology and Geodynamics*. Moscow, Nauka, 1986: 168-178 (*Comput. Seismol.*; Iss. 19, in Russian). English translation: *Computational Seismology*, Vol. 19, Allerton Press Inc., 1986: 168-177.
- Gabrielov, A.M., T.A. Levshina, and I.M. Rotwain (1990). Block model of earthquake sequence. *Phys. Earth and Planet. Inter.*, **61**: 18-28.
- Gabrielov, A., and W.I. Newman (1994). Seismicity modelling and earthquake prediction: A review. In W.I. Newman, A. Gabrielov, and D.L. Turcotte (eds), *Nonlinear Dynamics and Predictability of Geophysical Phenomena*. Am. Geophys. Un., Int. Un. of Geodesy and Geophys.: 7-13 (*Geophysical Monograph* 83, IUGG Vol. 18).
- Gabrielov, A., V. Kossobokov, and A. Soloviev (1994). Numerical simulation of block structure dynamics. In *Seismicity and Related Processes in the Environment*, Vol.1. Moscow, Research and Coordinating Centre for Seismology and Engineering: 22-32.
- Gabrielov, A., I. Zaliapin, W.I. Newman, and V.I. Keilis-Borok (2000). Colliding cascades model for earthquake prediction. *Geophys. J. Int.*, **143**, 2: 427- 437.
- Gasilov, V., V. Maksimov, V. Kossobokov, A. Prozorov, and A. Soloviev (1995). *Numerical Simulation of Block Structure Dynamics. II. Examples*. Third Workshop on Non-Linear Dynamics and Earthquake Prediction, 6 - 17 November 1995, Trieste, ICTP, H4.SMR/879-3, 48 pp.
- Gorshkov, A., and A. Soloviev (1996). The Western Alps: numerical modelling of block structure and seismicity. In *XXV General Assembly of ESC*, September 9-14, 1996, Reykjavik, Iceland, Abstracts: 66.
- Gorshkov, A., V. Keilis-Borok, I. Rotwain, A. Soloviev, and I. Vorobieva (1997). On dynamics of seismicity simulated by the models of blocks-and-faults systems. *Annali di Geofisica*, **XL**, 5: 1217-1232.
- Gripp, A.E., and Gordon, R.G. (1990). Current plate velocities relative to the hotspots incorporating the NUVEL-1 global plate motion model. *Geophysical Research Letters*, **17**, 8, 1109-1112.

- Hattori, S. (1974). Regional distribution of b-value in the world. *Bull. Intern. Inst. Seismol. and Earth Eng.*, **12**: 39-58.
- Ismail-Zadeh, A.T., Keilis-Borok, V.I., and Soloviev, A.A. (1999) Numerical modelling of earthquake flow in the south-eastern Carpathians (Vrancea): effect of a sinking slab. *Phys. Earth Planet. Inter.*, **111**, 3-4: 267-274.
- Keilis-Borok, V.I., and V.G. Kossobokov (1990). Premonitory activation of earthquake flow: algorithm M8. *Phys. Earth Planet. Inter.*, **61**, 1-2: 73-83.
- Keilis-Borok, V.I., I.M. Rotwain, and A.A. Soloviev (1997). Numerical modelling of block structure dynamics: dependence of a synthetic earthquake flow on the structure separateness and boundary movements. *J. Seismol.*, **1**: 151-160.
- Kronrod, T.L. (1984). Seismicity parameters of the main regions of the high seismic activity. In V.I. Keilis-Borok, and A.L. Levshin (eds), *Logical and Computational Methods in Seismology*. Moscow: Nauka: 36-57 (*Comput. Seismol.*; Iss.17, in Russian).
- Maksimov, V.I., and A.A. Soloviev (1999). Clustering of earthquakes in a block model of lithosphere dynamics. In D.K. Chowdhury (ed.), *Computational Seismology and Geodynamics 4*, Am. Geophys. Un., Washington, D.C., The Union: 124-126.
- Melnikova, L.A., V.L. Rozenberg, and A.A. Soloviev (1997). Numerical simulation of block-structure dynamics: the model with 3D movements of blocks. In Abstracts of XXII General Assembly of the European Geophysical Society, 21-25 April, Vienna, Austria, *Annales Geophysicae*, **15**, Supplement I, Part I: C174.
- Melnikova, L.A., V.L. Rozenberg, P.O. Sobolev, and A.A.Soloviev (2000). Numerical simulation of tectonic plate dynamics: a spherical block model. In V.I.Keilis-Borok and G.M.Molchan (eds), *Problems in Dynamics and Seismicity of the Earth*. Moscow, GEOS: 138-153 (*Comput. Seismol.*; Iss. 31, in Russian).
- Mocanu, V.I. (1993). *Final report "Go West" Programme*. Proposal No: 4609. Contract No: CIPA3510PL924609. Subject: "Methods for Investigation of Different Kinds of Lithospheric Plates in Europe". Period September-December 1993.
- Molchan, G., T. Kronrod, and G.F. Panza (1997). Multi-scale seismicity model for seismic risk. *Bulletin of the Seismological Society of America*, **87**, 5: 1220-1229.
- Narteau, C., P. Shebalin, M. Holschneider, J.-L. Le Mouél, and C.J. Allègre (2000). Direct simulations of the stress redistribution in the scaling organization of fracture tectonics (SOFT) model. *Geophys. J. Int.*, **141**, 1: 115-135.
- Newman, W.I., D.L. Turcotte, and A.M. Gabrielov (1995). Log-periodic behaviour of a hierarchical failure model with application to precursory seismic activation. *Phys. Rev. E*, **52**: 4827-4835.
- Panza, G.F., A.A. Soloviev, and I.A. Vorobieva (1997). Numerical modelling of block-structure dynamics: Application to the Vrancea region. *Pure Appl. Geophys.*, **149**: 313-336.
- Press,F., and C. Allen (1995). Patterns of seismic release in the southern California region. *J. Geophys. Res.*, **100**: 6421-6430.
- Prozorov, A.G. (1991). On the long range interaction among strong seismic events. In *Major Puzzling Problems or Paradoxes in Contemporary Geophysics*. IUGG-U3 Abstracts. Vienna, 1991: 29.
- Prozorov, A.G. (1993). Long range interaction of strong seismic events as a feature of intermittent character of plate dynamics. In *AGU Spring Meeting, May 24-28, Baltimore, Maryland*: 318 (*EOS Transactions*, AGU, **74**, 16/Supplement).
- Rotwain, I.M., and A.A. Soloviev (1998). Numerical modelling of block structure dynamics: temporal characteristics of a synthetic earthquake flow. In V.I.Keilis-Borok and G.M.Molchan (eds), *Problems in Geodynamics and Seismology*. Moscow, GEOS: 275-288 (*Comput. Seismol.*; Iss. 30, in Russian).

- Rozenberg, V., and A. Soloviev (1997). *Considering 3D Movements of Blocks in the Model of Block Structure Dynamics*. Fourth Workshop on Non-Linear Dynamics and Earthquake Prediction, 6 - 24 October 1997, Trieste, ICTP, H4.SMR/1011-3, 27 pp.
- Rundquist, D.V., and A.A. Soloviev (1999). Numerical modelling of block structure dynamics: an arc subduction zone. *Phys. Earth and Planet. Inter.*, **111**, 3-4: 241-252.
- Shaw, B.E., J.M. Carlson, and J.S. Langer (1992). Patterns of seismic activity preceding large earthquakes. *J. Geophys. Res.*, **97**: 479.
- Shebalin, P., I. Zaliapin, and V. Keilis-Borok (2000). Premonitory raise of the earthquakes' correlation range: Lesser Antilles. *Phys. Earth and Planet. Inter.*, **122**, 3-4: 241-249.
- Sobolev, P.O., A.A. Soloviev, and I.M. Rotwain (1999). Modelling of the lithosphere dynamics and seismicity for the Near East. In D.K. Chowdhury (ed.), *Computational Seismology and Geodynamics 4*, Am. Geophys. Un., Washington, D.C., The Union: 115-123.
- Soloviev, A.A. (1995). Modeling of block structure dynamics and seismicity. In *European Seismological Commission, XXIV General Assembly, 1994 September 19-24, Athens, Greece, Proceedings and Activity Report 1992-1994*, Vol.III. University of Athens, Faculty of Sciences, Subfaculty of Geosciences, Department of Geophysics & Geothermy: 1258-1267.
- Soloviev, A.A., V.L. Gasilov, V.I. Maksimov, and B.V. Digas (1996). 3D block model of lithosphere dynamics. In *Seismology in Europe, Papers presented at the XXV General Assembly of the European Seismological Commission*, Reykjavik, Iceland: 264-269.
- Soloviev, A.A., I.A. Vorobieva, and G.F. Panza (1999a). Modelling of block-structure dynamics: Parametric study for Vrancea. *Pure and Appl. Geophys.*, **156**, 3: 395-420.
- Soloviev, A., D.V. Rundquist, V.V. Rozhkova, and G.L. Vladova (1999b). *Application of Block Models to Study of Seismicity of Arc Subduction Zones*. Fifth Workshop on Non-Linear Dynamics and Earthquake Prediction, 4 - 22 October 1999, Trieste, ICTP, H4.SMR/1150-3, 31 pp.
- Soloviev, A., and I. Vorobieva (1999). Study of long-range interaction between synthetic earthquakes in the model of block structure dynamics. In *IUGG99, Birmingham, Abstracts, Week A, Monday 19 July to Saturday 24 July*: A.147.
- Soloviev, A.A., I.A. Vorobieva, and G.F. Panza (2000). Modelling of block structure dynamics for the Vrancea region: Source mechanisms of the synthetic earthquakes. *Pure and Appl. Geophys.*, **157**, 1-2: 97-110.
- Turcotte, D.L. (1997). *Fractals and Chaos in Geology and Geophysics*. 2nd Ed., Cambridge, University Press, 398 pp.
- Utsu, T., and A. Seki (1954). A relation between the area of aftershock region and the energy of main shock, *J. Seism. Soc. Japan*, **7**: 233-240.
- Vorobieva, I.A., A.I. Gorshkov, and A.A. Soloviev (2000). Modeling of the block structure dynamics and seismicity for the Western Alps. In V.I.Keilis-Borok and G.M.Molchan (eds), *Problems of Dynamics and Seismicity of the Earth*. Moscow, GEOS: 154-169 (Comput. Seismol.; Iss. 31, in Russian).
- Vorobieva, I.A., and A.A. Soloviev (2001). Long-range interaction between synthetic earthquakes in the model of lithosphere block dynamics. In G.M.Molchan, B.M.Naimark, and A.L.Levshin (eds), *Problems in Lithosphere Dynamics and Seismicity*. Moscow, GEOS: 202-211 (Comput. Seismol.; Iss. 32, in Russian).